NHERP AWARD 04HQGR0120
Final Technical Report

Earthquake Slip Distributions, Mechanics of Earthquake Rupture, and Seismic Hazard Analysis.

Steven G. Wesnousky
Center for Neotectonic Studies
University of Nevada, Reno
MS 169
Reno, NV 89557
775-784-6067 (tel), 775-784-1382 (fax)
stevew@seismo.unr.edu
http:// neotectonics.seismo.unr.edu

Program Element: NIW
Key words: neotectonics, paleseismology, fault mechanics, seismic hazard

Abstract

It has become standard practice during the last ~35 years to map the geometry of rupture traces and assess the surface-slip distribution of large earthquakes that break the ground surface. The resulting observations have been used in development of seismic hazard methodologies and assessments, engineering design criteria for critical facilities, the development and discussion of dynamic fault models to predict strong ground motions, and efforts to predict the endpoints of future earthquake ruptures. There now exist about 3 dozen historical earthquakes for which investigators have put forth maps of earthquake rupture traces with data describing the coseismic slip as a function of fault length. For this years work we have compiled and present here the surface rupture trace of each of the earthquakes. The compilation provides a foundation to begin quantitatively examining the role of geometrical discontinuities on the propogation of earthquake rupture. Our analysis shows that approximately 75% of the endpoints of strike-slip earthquake ruptures are associated with geometrical discontinuities, none of the earthquakes in the data set have ruptured through fault steps of 5 km or greater. When considering fault steps of lesser dimension along rupture traces, it is observed that about 40% are associated with the endpoints of rupture and the remainder are located within the rupture trace, effectively having been ruptured through by the respective rupture. There are fewer data available for dip-slip faults, though the few observations do show that normal fault ruptures have ruptured through fault discontinuities significantly greater than 5 km. These observations are important to the understanding of fault dynamics and the development of computer algorithms to estimate the extent of earthquake ruptures on mapped faults for seismic hazard analysis.

Introduction

Since the first studies of the 1968 Borrego Mountain [*Clark*, 1972] and 1857 Ft. Tejon [*Sieh*, 1978] earthquakes, it has become standard practice to map the geometry of rupture traces and assess the surface-slip distribution of large earthquakes that break the ground surface. The results of such studies have been a constant source of reference and use in development of seismic hazard methodologies [*Frankel et al.*, 2002; *Petersen and Wesnousky*, 1994; *SCEC*, 1994; *Wesnousky*, 1986; *Wesnousky et al.*, 1984], engineering design criteria for critical facilities [*Fuis and Wald*, 2003; *Kramer*, 1996; *Pezzopane and Dawson*, 1996], and development and discussion of mechanical models to understand physical factors that control the dynamics of the earthquake source as well as the resulting strong ground motions [*Bodin and Brune*, 1996; *Heaton*, 1990; *Romanowicz*, 1994; *Scholz*, 1994; *Scholz et al.*, 1986]. There now exist about 3 dozen historical earthquakes for which investigators have constructed maps of earthquake rupture traces accompanied by data describing the coseismic slip observed along fault strike. In this years work we have focused on the compilation and examination of the relationship of geometrical fault complexity to the endpoints of earthquake ruptures. The motivation has been to put on predictive footing the assessment of future earthquake rupture endpoints on mapped faults for seismic hazard analysis and place observational bounds on physical computer models of earthquake rupture. Examination of the earthquake slip distributions will be the next focus of study.

Method

We have limited our attention to the larger surface rupture earthquakes for which there exist both relatively detailed maps and measurements of coseismic offset along strike of the rupture. The earthquakes considered are listed in **Table 1**. Shown chronologically in **Figure 1** are maps of the surface rupture traces as presented by the original sources. Along the mapped fault traces, I have annotated the location of geometrical discontinuities along and at the ends of the earthquake ruptures, such as steps, splays, gaps in coseismic offsets along rupture traces, and distances to nearest neighboring active fault traces from the endpoints of surface rupture traces. The dimensions of steps measured perpendicular to fault strike and gaps in slip along fault strike are also noted. The resolution of the available maps generally limits observations to discontinuities of about 1 km and greater.

Observations and Implications

Fault Geometry and Endpoints of Earthquake Ruptures

Earthquakes of Strike-slip Mechanism

The majority of events surveyed are strike-slip. The relationship between the length of rupture and geometrical discontinuities along strike is summarized in the plot of **Figure 2**. The vertical axis is the dimension distance in kilometers. Along the horizontal axis, I have spaced evenly and ordered by increasing rupture length each of the strike-slip earthquakes. A dotted line extends vertically from each of the labeled earthquakes. Along each dotted line are plotted various symbols. The symbols denote the dimension of steps and gaps in surface rupture along strike and at the terminus of the respective ruptures. Separate symbols are used according to whether the steps are releasing or restraining in nature, and whether they occur within (rupture continues through) or at the endpoints of the rupture trace. In certain instances, the endpoints of rupture are not associated with a discontinuity in fault strike, in which the endpoint of rupture is

denoted by a separate symbol and annotated with the distance that the active trace continues beyond the endpoint of rupture. Also, because of the complexity of some ruptures and subparallel and branching fault traces, some earthquakes have more than two 'ends'.

That steps in fault trace may impede or arrest rupture propagation has been noted previously on the basis of both observational and theoretical grounds. The compilation of observations depicted in **Figure 2** indicates that about three fourths of terminations of strike-slip ruptures may be associated with geometrical steps in fault trace or the termination of the active fault on which they occurred (**Figure 3**). The histogram in **Figure 4** further expedites comparison of the dimensions of discontinuities through which ruptures have propagated to those that are located at the terminus of the earthquake ruptures. In this case, the observations of discontinuities are binned as a function of their size and coded according to whether they sit within or at the terminus of an earthquake rupture. The plot suggests to me that a transition exists between 3 and 5 km, above which rupture fronts are not able to propagate through and below which it is an pretty much even bet whether or not a rupture will continue or stop at a particular discontinuity. The result may be of practical importance in seismic hazard analysis where effort is spent attempting to place limits on the probable length of mapped active faults. One may surmise that the variability of behavior for steps below 3-4 km dimension in part reflects variability in the 3-dimensional character of the discontinuities we map at the surface. Some perhaps do not extend through the entirety of the seismogenic layer. Turning attention back to **Figure 2**, I further note that there appears to be no dependence on rupture length associated with the just mentioned transition. Longer ruptures are not observed to rupture or arrest at relatively larger discontinuities. The lack of rupture length dependence observed here leads me to suggest that, for an earthquake that has ruptured the entirety of the seismogenic layer, there exists no fundamental difference in the processes occurring at the fronts of propagating ruptures, regardless of the distance it has or will propagate.

Earthquakes of Normal Mechanism

The data for surface ruptures on normal faults is limited to 7 earthquakes. I follow the same approach as described for strike-slip faults to examine the relationship of the size and location of geometrical discontinuities to extent of earthquake surface rupture (**Figure 5**). The data in **Figure 5** are replotted in the form of a pie diagram in **Figure 6** whether or not the endpoints of the earthquake ruptures occur at fault discontinuities (**Figure 6**). About two thirds of the rupture endpoints correlate to the location of fault discontinuities. The data of **Figure 5** are yet further reformatted in the histogram of **Figure 7**. In this case, attention is limited to fault discontinuities, and the discontinuities are binned as a function of their size and coded according to whether they sit within or at the terminus of an earthquake rupture. Though the data are significantly fewer for normal faults and insufficient to draw a significant statistical conclusion, they do suggest a somewhat different relation as compared to strike-slip ruptures. Specifically, strike-slip earthquakes are generally not observed to rupture across discontinuities of 3 to 4 km whereas there are numerous instances of discontinuities of 4 km and greater through which normal faults have ruptured through or across. The slip vector of normal faults is orthogonal to the horizontal rupture direction in large earthquakes. Thus unlike for strike-slip ruptures there exist no volumetric considerations at the site of fault steps that lead to the possibility of localized stress changes. It is perhaps for this reason that geometrical discontinuities appear to play a relatively lesser role in affecting the propagation of earthquake ruptures.

Earthquakes of Thrust Mechanism

The data for thrust faults are also few, limited to 6 earthquakes. Again ordered by increasing rupture length, I have plotted the discontinuities through which ruptures have propagated and stopped, respectively (**Figure 8**). There are only two recorded instances of thrust ruptures propagating through mapped steps, of 2 and 6 km, respectively. In only one case is it clear that rupture terminated in the absence of a discontinuity. The remaining cases show termini associated with geometrical discontinuities, though the mapping available to me is insufficient to clearly characterize the dimension or character of the discontinuity along several of the earthquakes, in which case the symbols in Figure 8 are marked by queries.

Caveats, Other Factors, and Future Avenues of Research

I have limited attention to discontinuities that may be characterized by breaks in the fault trace. Bends in fault trace or the intersection points of fault splays may also affect the propagation characteristics of earthquakes. But, in each case, there is a greater difficulty in quantifying the relative size of the discontinuity or the potential effect of the discontinuity on rupture propagation. In the case of steps in strike-slip fault traces, it is clear that volumetric considerations resulting from displacement at the step will result in contractional or extensional stresses within the step, regardless of the direction of rupture propagation (**Figure 9a**). In the case of a single bend in strike-slip fault trace, more information than solely the geometry is required to understand the potential role of a bend on rupture propagation. For example, the stresses changes resulting from volumetric considerations at a bend may differ depending on the direction of rupture propagation (**Figure 9b**), in one case perhaps impeding rupture while in the other facilitating. The problem is perhaps voided if it is clear that the strike along one of the branches of the bend clearly defines the slip vector but, as noted, this requires additional information, perhaps subjective. The problem is yet further exacerbated because of the problem of scale. A bend may be defined by the angle but the potential interaction of a bend will also be a function of the length of the fault branches. For example, even though the bends of the fault in **Figure 9b** are the same, the effect on rupture propagation will certainly differ for the bends in **Figure 9b** depending on whether the fault branches are a 100 km long or 1 m long. In the case of a double bend along a strike-slip fault, the problem is somewhat obviated when the dominant slip direction is well known (**Figure 9c**). It is clear whether or not a branch will be under transpression or transtension due to the orientation of the bend. But there remains the problem of scale and the requirement that more than just the angle of the bend be used in defining the feature. The length of the fault branches must also play a role.

Splays and their intersection with faults likely also play a role in the characteristics of a propagating rupture. For example, the ends of the recent Nov 3, 2002 Denali earthquake are associated with intersection of the Susitna Gacier reverse and Totschunda strike-slip splay faults with the Denali fault. But the quantification of the potential relative effect of splay faults other than that they exist is also problematic and the data set to examine this issue is limited relative to that available for studying fault steps.

That the location of recent earthquake ruptures commonly defines or controls the edges of future earthquake ruptures has been well demonstrated along the subduction zones of the globe. There seems little doubt that such information may also serve in defining the extent of future earthquake ruptures. The historical sequence of earthquake surface ruptures along the Anatolian provides support for the same to be true for continental earthquakes. The historical data set of earthquake surface ruptures (**Figure 1**) is currently insufficient to examine this in more than an anecdotal manner, though it seems that such data be among the most important in defining the extent of future earthquake ruptures along mapped active faults.

When categorizing the location of geometrical discontinuities with respect to the endpoints of rupture, I have not considered the variation of slip along the ends of faults. In certain instances, the terminal sections of fault rupture are characterized by very small amounts of slip and arguably only represent minor triggered slip. Strands at the northern and southern ends of the 1992 Landers earthquake are cases in point. Most of the moment release clearly occurred in the central portions of the fault zone. The results conveyed in **Figures 2** through **8** might change slightly were the terminal ends of nominal slip not considered and the endpoints of rupture redefined. However, the interpretation in some instances would be quite subjective and for that reason I have not done so in this effort.

Discussion and Conclusion

The record of historical earthquake ruptures is becoming sufficient to put forth some general rather than anecdotal conclusions regarding the role of geometrical discontinuities in earthquake rupture process. These initial observations indicate that about 75% of the endpoints of earthquake ruptures are associated with geometrical steps in fault trace or the endpoints of mapped faults. Of those 75%, it is observed that fault steps of 5 km or more are of dimension sufficient to consistently arrest strike-slip earthquake ruptures, while discontinuities of lesser dimension are associated with the endpoints of rupture in only about 40% of the cases. The lesser correlation of fault endpoints with smaller steps probably reflects both the smaller dimension of the steps and the liklihood that smaller fault steps observed at the surface do maintain their form or integrity through the entirety of the seismogenic layer. Data are insufficient to place percentage bounds of any significance for dip-slip faults, though it is recognized that normal fault ruptures have historically ruptured through fault steps of larger dimension than strike-slip faults

References

Abe, K. (1978), Dislocations, source dimensions and stresses associated with earthquakes in the Izu Peninusula, Japan, *Journal of Physics of the Earth*, *26*, 253-274.

Akyuz, H. S., et al. (2002), Surface rupture and slip distribution of the 12 November 1999 Duzce Earthquake (M 7.1), North Anatolian Fault, Bolu, Turkey, *Bulletin of Seismological Society of America*, *92*, 61-66.

Anderson, H., and T. Webb (1989), The rupture process of the 1987 Edgecumbe earthquake, New Zealand, *New Zealand Journal of Geology and Geophysics*, *32*, 43-52.

Ando, M. (1974), Faulting in the Mikawa earthquake of 1945, *Tectonophysics*, *22*, 173-186.

Antolik, M., et al. (2004), The 14 November 2001 Kokoxili (Kunlunshan), Tibet, earthquake: Rupture transfer through a large extensional step-over, *Bulletin of the Seismological Society of America*, *94*, 1173-1194.

Barka, A. (1996), Slip distribution along the North Anatolian Fault associated with the large earthquakes of the period 1939 to 1967, *Bulletin of Seismological Society of America*, *86*, 1238-1254.

Barka, A., et al. (2002), The surface rupture and slip distribution of the 17 August 1999 Izmit Earthquake (M 7.4), North Anatolian Fault, *Bulletin of Seismological Society of America*, *92*, 43-60.

Barrientos, S. E., et al. (1987), Comparison of the 1959 Hebgen Lake, Montana and the 1983 Borah Peak, Idaho, earthquakes from geodetic observations, *Bulletin of the Seismological Society of America*, *77*, 784-808.

Beanland, S., et al. (1989), Geological investigations of the 1987 Edgecumbe earthquake, New Zealand, *New Zealand Journal of Geology and Geophysics*, *32*, 73-91.

Bodin, P., and J. N. Brune (1996), On the scaling of slip with rupture length for shallow strike-slip earthquakes: Quasi-static models and dynamic rupture propagation, *Bulletin of the Seismological Society of America*, *86*, 1292-1299.

Bull, W. B., and P. A. Pearthree (2002), Frequency and size of Quaternary surface ruptures of the Pitaycahic fault, northeastern Sonora, Mexico, *Bulletin of the Seismological Society of America*, *78*, 956-978.

Burdick, L., and G. R. Mellman (1976), Inversion of the body waves from the Borrego Mountain earthquake to source mechanism, *Bulletin of the Seismological Society of America*, *66*, 1485-1499.

Burgmann, R., et al. (2002), Deformation during the 12 November 1999 Duzce, Turkey, earthquake, from GPS and Insar data, *Bulletin of the Seismological Society of America*, *92*, 161-171.

Butler, R. (1983), Surface wave analysis of the 9 April 1968 Borrego mountain earthquake, *Bulletin of the Seismological Society of America*, *73*, 879-883.

Caskey, S. J., et al. (1996), Surface faulting of the 1954 Fairview Peak (Ms=7.2) and Dixie Valley (Ms=6.8) earthquakes, central Nevada., *Bulletin of the Seismological Society of America*, *86*, 286-291.

Chi, W. C., et al. (2001), Finite-source modeling of the 1999 Taiwan (Chi-Chi) earthquake derived from a dense strong-motion network, *Bulletin of the Seismological Society of America*, *91*, 1144-1157.

Choy, G. L., and J. Boatwright (2004), Radiated energy and the rupture process of the Denali fault earthquake sequence of 2002 from broadband teleseismic body waves, *Bulletin of the Seismological Society of America*, *94*, S269-S277.

Choy, G. L., and J. R. Bowman (1990), Rupture process of a multiple main shock sequence; analysis of teleseismic, local, and field observations of the Tennant Creek, Australia, earthquakes of Jan 22, 1988, *Journal of Geophysical Research*, *95*, 6867-6882.

Clark, M. M. (Ed.) (1972), *Surface rupture along the Coyote Creek fault, the Borrego Mountain Earthquake of April 9, 1968*, 55-86 pp., United States Geological Survey.

Cohee, B. P., and G. c. Beroza (1994), Slip distribution of the 1992 landers earthquake and its implications for earthquake source mechanics, *Bulletin of the Seismological Society of America*, *84*, 692-712.

Crone, A., et al. (1987), Surface faulting accompanying the Borah Peak earthquake and segmentation of the Lost River Fault, central Idaho, *Bulletin of Seismological Society of America*, *77*, 739-770.

Crone, A. J., et al. (1992), Geologic Investigations of the 1988 Tennant Creek, Australia, Earthquakes - Implications for paleoseismicity in stable continental regions, *United States Geological Survey Bulletin*, *2032-A*, A1-A51.

Delouis, B., et al. (2002), Joint inversion of InSAR, GPS, Teleseismic, and Strong-motion data for the spatial and temporal distribution of earthquake slip: application to the 1999 Izmit mainshock, *Bulletin of the Seismological Society of America*, *92*, 278-299.

Doser, D. I. (1985), Source parameters and faulting processes of the 1959 Hebgen lake, Montana, earthquake sequence, *Journal of Geophysical Research*, *90*, 4537-4555.

Doser, D. I. (1986), Earthquake processes in the Rainbow Mountain-Fairview Peak-Dixie Valley, Nevada, region 1954-1959, *Journal of Geophysical Research*, *91*, 12572-12586.

Doser, D. I. (1988), Source parameters of earthquakes in the Nevada seismic zone, 1915-1943, *Journal of Geophysical Research*, *93*, 15001-15015.

Doser, D. I. (1990), Source characteristics of earthquakes along the southern San Jacinto and Imperial fault zones (1937 to 1954), *Bulletin of the Seismological Society of America*, *80*, 1099-1117.

Doser, D. I., and H. Kanamori (1987), Long period surface waves of four western United States earthquakes recorded by the Pasadena strainmeter, *Bulletin of the Seismological Society of America*, *77*, 236-243.

Doser, D. I., and R. B. Smith (1985), Source parameters of the 28 October 1983 Borah Peak, Idaho, earthquake from body wave analysis, *Bulletin of the Seismological Society of America*, *75*, 1041-1051.

Dreger, D. (1994), Investigation of the rupture process of the 28 June 1992 landers earthquake utilizing TERRAscope, *Bulletin of the Seismological Society of America*, *84*, 713-724.

Dziewonki, A. M., et al. (1989), Centroid-moment tensor solutions for October-December 1987, *Physics of Earth and Planetary Interiors*, *54*, 10-21.

Ebel, J. E., and D. V. Helmberger (1982), P-wave complexity and fault asperities: the Borrego Mountain, California, earhquake of 1968, *Bulletin of the Seismological Society of America*, *72*, 413-437.

Frankel, A. (2004), Rupture process of the M 7.9 Denali fault, Alaska, earthquake: Subevents, directivity, and scaling of high-frequency ground motions, *Bulletin of the Seismological Society of America*, *94*, S234-S255.

Frankel, A., and L. Wennerberg (1989), Ruture process of the Ms 6.6 Superstition Hills earthquake determined from strong-motion recordings: application of tomographic source inversion, *Bulletin of the Seismological Society of America*, *79*, 515-541.

Frankel, A. D., et al. (2002), Documentation for the 2002 update of the national seismic hazard maps, *USGS Open-File Report*, *OF 02-0420*, 33 pp.

Fredrich, J., et al. (1988), Source parameters of seven large Australian earthquakes determined by body waveform inversion, *Geophysical Journal of the Royal Astronomical Society*, *95*, 1-13.

Freymueller, J. (1994), The co-seismic slip distribution of the Landers earthquake, *Bulletin of the Seismological Society of America*, *84*, 646-659.

Fuis, G. S., and L. A. Wald (2003), Rupture in south-central Alaska - The Denali fault earthquake of 2002, *U. S. G. S. Fact Sheet*, *014-03*, 4 p.

Haeussler, P. J., et al. (2005), Surface rupture and slip distribution of the Denali and Totschunda faults in the 3 November 2002 M7.9 earthquake, Alaska, *Bulletin of the Seismological Society of America*, *94*, S23-252.

Hanks, T. C., and M. Wyss (1972), The use of body-wave spectra in determination of seismic-source parameters, *Bulletin of the Seismological Society of America*, *62*, 561-589.

Hartzell, S. H., and T. Heaton (1983), Inversion of strong groundmotion and teleseismic waveform data for the fault rupture history of the 1979 Imperial Valley, California, earthquake sequence, *Bulletin of the Seismological Society of America*, *73*, 1553-1584.

Hartzell, S. H., and D. V. Helmberger (1982), Strong-motion modeling of the Imperial Valley earthquake of 1979, *Bulletin of the Seismological Society of America*, *72*, 571-596.

Heaton, T., and D. V. Helmberger (1977), A study of the strong ground motion of the borrego Mountain, California earthquake, *Bulletin of the Seismological Society of America*, *67*, 315-330.

Heaton, T. H. (1990), Evidence for and implication of self-healing pulses of slip in earthquake rupture, *Physics of the Earth and Planetary Interiors*, *64*, 1-20.

Hodgkinson, K. M., et al. (1996), Geometry of the 1954 Fairview Peak-Dixie Valley earthquake sequence from a joint inversion of leveling and triangulation data, *Journal of Geophysical Research*, *101*, 25437-25457.

Hwang, L. J., et al. (1990), Teleseismic source parameters and rupture characteristics of the 24 November 1987, Superstition Hills earthquake, *Bulletin of the Seismological Society of America*, *80*, 43-56.

Ji, C., et al. (2002), Source description of the 1999 Hector Mine, California, earthquake, Part I: Wavelet domain inversion theory and resolution analysis, *Bulletin of the Seismological Society of America*, *92*, 192-1207.

Johnson, C. E., and L. K. Hutton (1982), Aftershocks and Preearthquake Seismicity in 'The Imperial Valley California, Earthquake of October 15, 1979, *United States Geological Survey Professional Paper*, *1254*, 59-76.

Johnson, H. O., et al. (1994), Extremal bounds on earthquake movement from geodetic data - application to the Landers earthquake, *Bulletin of the Seismological Society of America*, *84*, 660-667.

Jonsson, S., et al. (2002), Fault slip distribution of the 1999 Mw 7.1 Hector Mine, California earthquake, etimated from satellite radar and gps measurements, *Bulletin of the Seismological Society of America*, *92*, 1377-1389.

Kakehi, Y., and T. Iwata (1992), Rupture process of the 1945 Mikawa earthquake as determined from strong ground motion records, *Journal of Physics of the Earth*, *40*, 635-655.

Kanamori, H. (1973), Mode of strain release associated with major earthquakes in Japan, *Annual Review of Earth and Planetary Sciences*, *1*, 213-239.

Kanamori, H., and J. Reagan (1982), Long-period surface waves, *U.S. Geological Survey Professional Paper*, *1254*, 55-58.

Kaneda, H., and A. Okada (2002), Surface rupture associated with the 1943 Tottori earthquake: compilation of previous reports and its tectonic geomorphological implications, *Active Fault Research*, *21*, 73-91 (in Japanese with English Abstract).

Kaverina, A., et al. (2002), The combined inversion of seismic and geodetic data for the source process of the 16 ctober 1999 Mw 7.1 Hector Mine, earthquake, *Bulletin of the Seismological Society of America*, *92*, 1266-1280.

Kikuchi, M., et al. (2003), Source rupture processes of the 1944 Tonankai earthquake and the 1945 Mikawa earthquake derived from low-gain seismograms, *Earth Planets and Space*, *55*, 159-172.

Klinger, Y., et al. (2005), High-resolution satellite imagery mapping of the surface rupture and slip distribution of the Mw ~7.8, 114 November 2001 Kokoxili earthquake, Kunlun fault, northern Tibet, China, *Bulletin of the Seismological Society of America*, *95*, 1970-1987.

Kramer, S. L. (1996), *Geotechnical earthquake engineering*, 653 pp., Prentice Hall, Upper Saddle River, N. J.

Larsen, S., et al. (1992), Global positioning system measurements of deformations associated with the 1987 Superstition Hills earthquake, *Journal of Geophysical Research*, *97*, 4885-4902.

Lasserre, C., et al. (2005), Coseismic deformation of the 2001 M-w=7.8 Kokoxili earthquake in Tibet, measured by synthetic aperture radar interferometry, *Journal of Geophysical Research-Solid Earth*, *110*.

Li, X., et al. (2002), Complex source process of the 17 August 1999 Izmit, Turkey, earthquake, *Bulletin of the Seismological Society of America*, *92*, 267-277.

Lin, A., et al. (2002), Co-seismic strike-slip and rupture length produced by the 2001 Ms 8.1 central Kunlun earthquake, *Science*, *296*, 2015-2017.

Lin, A., et al. (2001), Co-seismic displacements, folding and shortening structures along the Chelungpu surface rupture zone occurred during the 1999 Chi-Chi (Taiwan) earthquake, *Tectonophysics*, *330*, 225-244.

Machette, M. N., et al. (1993), Geologic investigations of the 1986 Marryat Creek, Australia, earthquake - implications for paleoseismicity in stable continental regions, *United States Geological Survey Bulletin*, *2032 B*, p. 29p.

Matsuda, T. (1972), Surface faults associated with Kita-Izu Earthquake of 1930 in Izu Peninsula, Japan, in *Izu Peninsula*, edited by M. Hoshino and H. Aoki, pp. 73-102., Tokai University Press, Tokyo.

Matsuda, T. (1974), Surface faults associated with Nobi (Mino-Owari) Earthquake of 1891, Japan, *Bulletin of Earthquake Research Institute, University of Tokyo*, *13*, 127-162.

Matsuda, T., et al. (1980), The surface faults associated with the Rikuu Earthquake of 1896, *Bulletin of Earthquake Research Institute, University of Tokyo*, *55*, 795-855.

Mendoza, C., and S. H. Hartzell (1988), Inversion for slip distribution using teleseismic P waveforms: North Palm Springs, Borah Peak, and Michoacan earthquakes., *Bulletin of the Seismological Society of America*, *78*, 1092-1111.

Nakata, T. (1990), Surface faulting associated with the Philippine earthquake of 1990 (in Japanese), *Journal of Geography*, *99*, 95-112.

Ozacar, A. A., and S. L. Beck (2004), The 2002 Denali fault and 2001 Kunlun fault earthquakes: Complex rupture processes of two large strike-slip events, *Bulletin of the Seismological Society of America*, *94*, S278-S292.

Petersen, M. D., and S. G. Wesnousky (1994), Fault Slip Rates and Earthquake Histories for Active Faults in Southern California, *Bulletin of the Seismological Society of America*, *84*, 1608-1649.

Pezzopane, S. K., and T. E. Dawson (1996), Fault displacement hazard: A summary of issues and information, in *Seismotectonic Framework and Characterization of Faulting at Yucca Mountain*, edited by J. W. Whitney, pp. 9-1 - 9-160.

Pinar, A., et al. (1996), A rupture model for the 1967 Mudurnu Valley, Turkey earthquake and its implication for seismotectonics in the western part of the North anatolian fault zone, *Geophysical Research Letters*, *23*, 29-32.

Priestly, K. F. (1987), Source parameters of the 1987 Edgecumbe earthquake, New Zealand, *New Zealand Journal of Geology and Geophysics*, *32*, 53-59.

Reilinger, R. (1984), Coseismic and postseismic vertical movements associated with the 1940 M 7.1 Imperial Valley, California, earthquake, *Journal of Geophysical Research*, *89*.

Romanowicz, B. (1994), Comment on "A reappraisal of large earthquake scaling", *Bulletin of the Seismological Society of America*, *84*.

SCEC, W. G. (1994), Seismic Hazards in Southern California: Probable Earthquakes, 1994-2024, *Bulletin of the Seismological Society of America*, *85*, 379-439.

Scholz, C. H. (1994), Reply to comment on"A reapprasial of large earthquake scaling", *Bulletin of the Seismological Society of America*, *84*, 1677-1678.

Scholz, C. H., et al. (1986), Scaling differences between large interplate and intraplate earthquakes, *Bulletin of the Seismological Society of America*, *76*, 65-70.

Sekiguchi, H., and T. Iwata (2002), Rupture process of the 199 Kocaeli, Turkey, earthquake estimated from strong motion waveforms, *Bulletin of the Seismological Society of America*, *92*, 300-311.

Sharp, R., et al. (1989), Surface faulting along the Superstition Hills fault zone and nearby faults associated with the earthquakes of 24 November 1987, *Bulletin of Seismological Society of America*, *79*, 252-281.

Sharp, R., et al. (1982), Surface faulting in the Central Imperial Valley in 'The Imperial Valley California, Earthquake of October 15, 1979, *United States Geological Survey Professional Paper*, *1254*.

Sieh, K., et al. (1993), Near-field investigations of the Landers earthquake sequence, April to July 1992, *Science*, *260*, 171-176.

Sieh, K. E. (1978), Slip along the San Andreas Fault associated with the great 1857 earthquake, *Bulletin of the Seismological Society of America*, *68*, 1421-1448.

Sipkin, S. A. (1989), Moment-tensor solutions for the 24 November 1987 Superstition Hills, California earthquake, *Bulletin of the Seismological Society of America*, *79*, 493-499.

Stewart, G. S., and H. Kanamori (1982), Complexity of rupture in large strike-slip earthquakes in Turkey, *Physics of Earth and Planetary Interiors*, *28*, 70-84.

Suter, M., and J. Contreras (2002), Active tectonics of northeastern Sonora, Mexico (southern Basin and Range Province) and the 3 May 1887 Mw 7.4 Earthquake, *Bulleting of the Seismological Society of America*, *92*, 581-589.

Swanger, H. J., et al. (1978), Simulation of strong-motion displacements using surface-wave modal superposition, *Bulletin of the Seismological Society of America*, *68*, 907-922.

Tanimoto, T., and H. Kanamori (1986), Linear programming approach to moment tensor inversion of earthquake sources and some tests on the three-dimensional structure of the upper mantle, *Geophy. J. R. Astron. Soc.*, *84*, 413-430.

Taymaz, T., et al. (1991), Active tectonics of the north and central Aegean sea, *Geophy. J. Int.*, *108*, 589-603.

Thatcher, W., and T. C. Hanks (1973), Source parameters of southern California earthquakes, *Journal of Geophysical Research*, *78*, 8547-8576.

Treiman, J., et al. (2002), Primary surface rupture associated with the Mw 7.1 16 October 1999 Hector Mine earthquake, San Bernardino County, California, *Bulletin of the Seismological Society of America*, *92*, 1171-1191.

Trifunac, M. D. (1972), Tectonic stress and the source mechanism of the Imperial Valley, California, earthquake of 1940, *Bulletin of the Seismological Society of America*, *62*, 1283-1302.

Trifunac, M. D., and J. Brune (1970), Complexity of energy release during the Imperial Valley, California, earthquake of 1940, *Bulletin of Seismological Society of America*, *60*, 137-160.

Tsuya, K. (1946), The Fukozu fault. A remarkable earthquake fault formed during the Mikawa earthquake of January 13, 1945., *Bull. Earthquake Research Institute, Tokyo University*, *24*, 59-76 (in Japanese with English abstract).

Umutlu, N., et al. (2004), The rupture process during the 1999 Duzce, Turkey, earthquake from joint inversion of teleseismic and strong-motion data, *Tectonophysics*, *391*, 315-324.

Velasco, A. A., et al. (1996), Rupture process of the 1990 Luzon, Phillippines (Mw=7.7) earthquake, *Journal of Geophysical Research*, *101*, 22419-22434.

Vidale, J., et al. (1985), Finite difference seismograms for SH waves, *Bulletin of the Seismological Society of America*, *75*, 1765-1782.

Wald, D. J., and T. Heaton (1994), Spatial and temporal distribution of slip for the 1992 Landers, California, earthquake, *Bulletin of the Seismological Society of America*, *84*, 668-691.

Wald, D. J., et al. (1990), Rupture process of the 1987 Superstition Hills earthquake from the inversion of strong-motion data, *Bulletin of the Seismological Society of America*, *80*, 1079-1098.

Wallace, R. E. (1980), Map of fault scarps formed during earthquake of October 2, 1915, Pleasant Valley, Nevada, and other young fault scarps, in *U.S. Geological Survey Open File Report*, edited, U. S. Geological Survey, Reston, VA.

Ward, S. N., and S. E. Barrientos (1986), An inversion for slip distribution and fault shape from geodetic observations of the 1983 Borah Peak, Idaho, earthquake, *Journal of Geophysical Research*, *91*, 4909-4919.

Wesnousky, S. G. (1986), Earthquakes, Quaternary faults, and seismic hazard in California, *Journal of Geophysical Research*, *91*, 12,587-512,631.

Wesnousky, S. G., et al. (1984), Integration of geological and seismological data for the analysis of seismic hazard: A case study of Japan, *Bulletin of the Seismological Society of America*, *74*, 687-708.

Witkind, I. J. (1964), Reactivated faults north of Hebgen Lake, *U.S. Geological Survey Professional Paper*, *435-G*, 37-50.

Wu, C. J., et al. (2001), Source process of the Chi-Chi earthquake: a joint inversion of strong motion data and global positioning system data with multifault model, *Bulletin of the Seismological Society of America*, *91*, 1128-1143.

Xu, X., et al. (2002), Surface rupture of the Kunlunshan earthquake (Ms 8.1), northern Tibetan plateau, China, *Seismological Research Letters*, *73*, 884-892.

Yomogida, K., and T. Nakata (1994), Large slip velocity of the surface ruptures associated with the 1990 Luzon earthquake, *Geophysical Research Letters*, *21*, 1799-1802.

Yoshida, Y., and K. Abe (1992), Source Mechanism of the Luzon, Philippines earthquake of July 16, 1990, *Geophysical Research Letters*, *19*, 545-548.

Zeng, Y., and C. H. Chen (2001), Fault rupture process of the 20 September 1999 Chi-Chii, Taiwan earthquake, *Bulletin of the Seismological Society of America*, *91*, 1088-1098.

Table 1: Earthquake Surface Rupture Earthquakes

#	Date	Location	Type	Length (km)	M_w^g	Ref
1	1857-Jan-9	San Andreas, CA	ssr	360	7.9	1
2	1887-May-3	Sonora, MX	n/60	70	7.2	2,3,48
3	1891-Oct-28	Neo-Dani, JPN	ssl	80	7.3	4
4	1896-Aug-31	Rikuu, JPN	r/45	37	7.2	5
5	1915-Oct-2	Pleasant Val, NV	n/45	61	7.3	6
6	1930-Nov-2	Kita-Izu, JPN	ssl	35	6.7	7
7	1939-Dec-25	Erzincan, TUR	ssr	300	7.7	8
8	1940-May-19	Imperial, CA	ssr	60	6.9	9
9	1942-Dec-20	Erbaa-Niksar, TUR	ssr	28	6.8	8
10	1943-Nov-26	Tosya, TUR	ssr	275	7.5	8
11	1943-Sep-10	Tottori, JPN	ssl	10.5	6.2	10
12	1944-Feb-01	Gerede-Bolu, TUR	ssr	135	7.3	8
13	1945-Jan-31	Mikawa, JPN	r/30	4.5	6.3	11
14	1959-Aug-17	Hebgen Lake, MT	n/50	25	7.0	12
15	1954-Dec-16	Fairview Peak, NV	nssr/60	62	7.0	13
16	1954-Dec-16	Dixie Valley, NV	n/60	47	6.8	13
17	1967-Jul-22	Mudurnu, TUR	ssr	60	6.9	8
18	1968-Apr-8	Borrego Mtn, CA	ssr	31	6.1	14
19	1979-Jun-02	Cadoux, AUS	r/35	10	6.1	49
20	1979-Oct-15	Imperial, CA	ssr	36	6.2-6.4	15,16
21	1981-Jul-29	Sirch Iran	ss/69	64	6.2	50
22	1983-Oct-28	Borah Peak, ID	n/45	34	6.9	17
23	1986-Mar-3	Marryat, AUS	r/35	13	5.6(s) 5.9(u)	46
24	1987-Nov-23	Superstition Hills, CA.	ssr	25	6.2-6.4	18
25	1987-Mar-2	Edgecumbe, NZ	n/60	15.5	6.3	19
26	1988-Jan-22	Tennant Creek, AUS	r/45	30	6.0	43
27	1990-Jul-16	Luzon, PHL	ssl	112	6.9	20,21
28	1992-Jun-28	Landers, CA	ssr	77	7.2	22
29	1998-Mar-14	Fandoqa, IRN	ssn/54	25	6.6	50
30	1999-Sep-21	Chi-Chi, Taiwan	r/70	72	7.3	23
31	1999-Oct-16	Hector Mine, CA.	ssr	44	6.9	57
32	1999-Aug-17	Izmit, TUR	ssr	107 (145)	7.1	47
33	1999-Nov-12	Duzce, TUR	ssr	40	7.0	24
34	2001-Nov-14	Kunlun, China	ssl	421	7.8	53
35	2002-Nov-03	Denali, AK (Haessler)	ssr	302	7.6	52
#	Date	Location	Type	Length	M_w^g	Ref

1. [Sieh, 1978] , 2. [Bull and Pearthree, 2002], 3. [Pezzopane and Dawson, 1996], 4. [Matsuda, 1974], 5. [Matsuda et al., 1980], 6. [Wallace, 1980], 7. [Matsuda, 1972], 8. [Barka, 1996], 9. [Trifunac and Brune,

1970], 10. [Kaneda and Okada, 2002], 11. [Tsuya, 1946], 12. [Witkind, 1964], 13. [Caskey et al., 1996], 14. [Clark, 1972], 15. [Johnson and Hutton, 1982]] , 16. [Sharp et al., 1982] , 17. [Crone et al., 1987], 18. [Sharp et al., 1989], 19. [Beanland et al., 1989] , 20. [Nakata, 1990], 21. [Yomogida and Nakata, 1994], 22. [Sieh et al., 1993], 23. [Lin et al., 2001], 24. [Akyuz et al., 2002] , 25. [Cohee and Beroza, 1994; Dreger, 1994; Freymueller, 1994; Johnson et al., 1994; Wald and Heaton, 1994], 26. [Chi et al., 2001; Wu et al., 2001; Zeng and Chen, 2001] , 27. [Doser, 1988], 28. [Burdick and Mellman, 1976; Butler, 1983; Ebel and Helmberger, 1982; Hanks and Wyss, 1972; Heaton and Helmberger, 1977; Swanger et al., 1978; Vidale et al., 1985], 29. [Doser and Smith, 1985; Hanks and Wyss, 1972; Mendoza and Hartzell, 1988; Tanimoto and Kanamori, 1986; Ward and Barrientos, 1986], 30. [Doser, 1990; Hartzell and Heaton, 1983; Hartzell and Helmberger, 1982; Kanamori and Reagan, 1982], 31. [Barrientos et al., 1987; Doser and Kanamori, 1987; Doser and Smith, 1985], 32. [Velasco et al., 1996; Yoshida and Abe, 1992], 33. [Dziewonki et al., 1989; Frankel and Wennerberg, 1989; Hwang et al., 1990; Larsen et al., 1992; Sipkin, 1989; Wald et al., 1990], 34. [Anderson and Webb, 1989; Priestly, 1987] , 35. [Doser, 1986; Hodgkinson et al., 1996], 36. [Doser, 1985; Hodgkinson et al., 1996], 37. [Burgmann et al., 2002; Umutlu et al., 2004], 38. [Delouis et al., 2002; Li et al., 2002; Sekiguchi and Iwata, 2002] , 39. [Hanks and Wyss, 1972; Pinar et al., 1996; Stewart and Kanamori, 1982; Taymaz et al., 1991] , 40. [Kanamori, 1973] , 41. [Ando, 1974; Kakehi and Iwata, 1992; Kikuchi et al., 2003] , 42. [Doser, 1990; Doser and Kanamori, 1987; Reilinger, 1984; Thatcher and Hanks, 1973; Trifunac, 1972] , 43. [Crone et al., 1992] , 44. [Choy and Bowman, 1990] , 45. [Fredrich et al., 1988] , 46. [Machette et al., 1993] , 47. [Barka et al., 2002] , 48. [Suter and Contreras, 2002] , 49.[Lewis, 1981 #127] , 50. [Berberian, 2001 #128] , 51. [Eberhart-Phillips, 2003 #129] , 52. [Haeussler et al., 2005] , 53. [Klinger et al., 2005; Lin et al., 2002; Xu et al., 2002] , 54. [Choy and Boatwright, 2004; Frankel, 2004; Ozacar and Beck, 2004] , 55. [Antolik et al., 2004; Lasserre et al., 2005; Ozacar and Beck, 2004] , 56. [Abe, 1978], 57. [Treiman et al., 2002], 58. [Ji et al., 2002; Jonsson et al., 2002; Kaverina et al., 2002]

Figures

Figure 1. Maps of rupture traces and surface slip distributions for historical earthquake of (a) strike-slip, (b) normal, and (c) reverse mechanism considered in this study. Listing for each is chronological chronological. Sources for each are listed in **Table 1**. See text for further explanation.

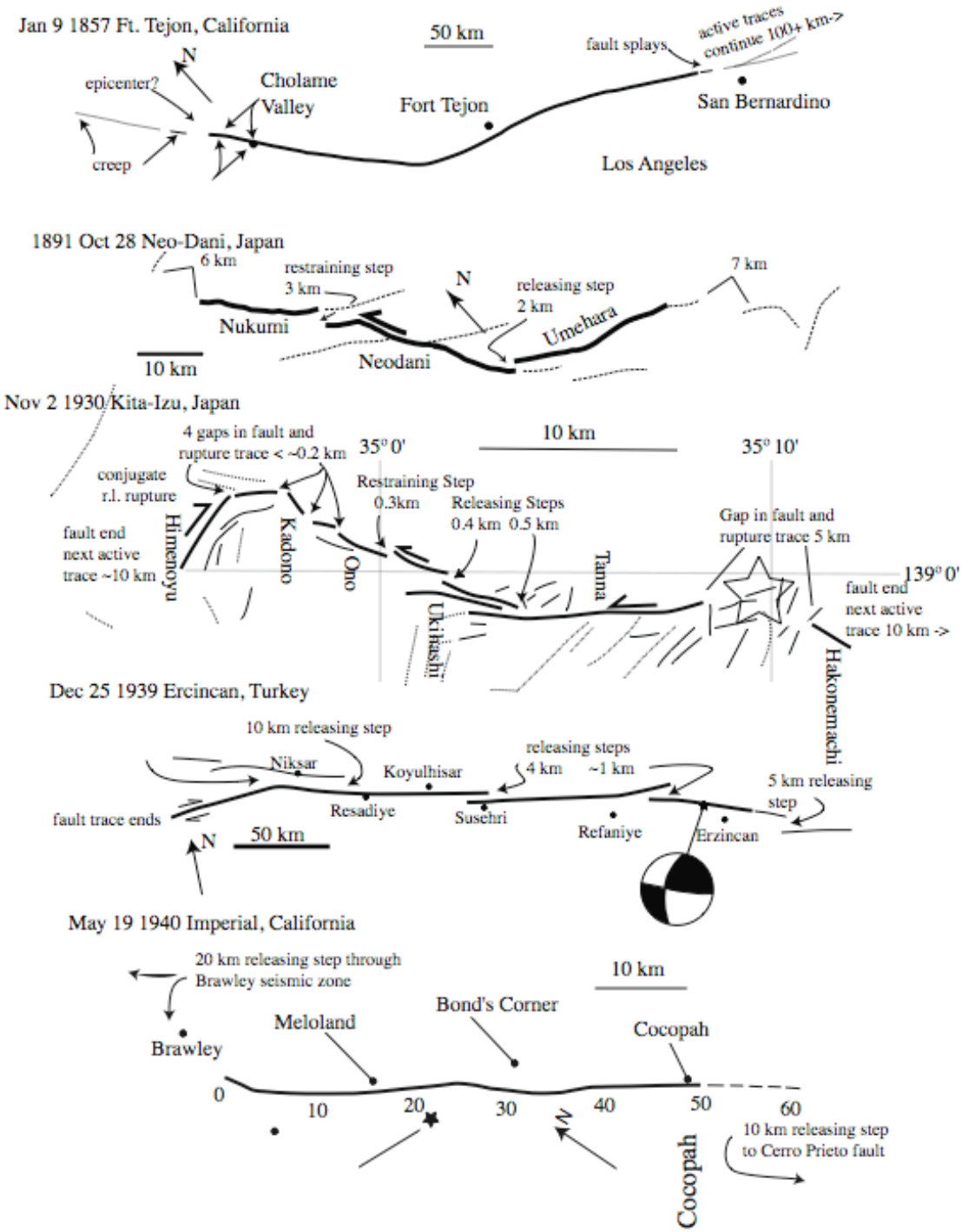
Jan 9 1857 Ft. Tejon, California
50 km
N
epicenter?
Cholame
Valley
Fort Tejon
fault splays
active traces
continue 100+ km->
San Bernardino
creep
Los Angeles
1891 Oct 28 Neo-Dani, Japan
6 km
restraining step
3 km
N
releasing step
2 km
7 km
Nukumi
Umehara
10 km
Neodani
Nov 2 1930 Kita-Izu, Japan
4 gaps in fault and
rupture trace < ~0.2 km
35° 0'
10 km
35° 10'
conjugate
r.l. rupture
Restraining Step
0.3km
Releasing Steps
0.4 km 0.5 km
Gap in fault and
rupture trace 5 km
fault end
next active
trace ~10 km
Himenoyu
Kadono
Ono
Tanna
139° 0'
fault end
next active
trace 10 km ->
Ukihashi
Hakonemachi
Dec 25 1939 Ercincan, Turkey
10 km releasing step
Niksar
Koyulhisar
releasing steps
4 km ~1 km
5 km releasing
step
fault trace ends
Resadiye
Susehri
Refaniye
Erzincan
N
50 km
May 19 1940 Imperial, California
20 km releasing step through
Brawley seismic zone
10 km
Bond's Corner
Meloland
Cocopah
Brawley
0
10
20
30
40
50
60
N
10 km releasing step
to Cerro Prieto fault
Cocopah

Figure 1a

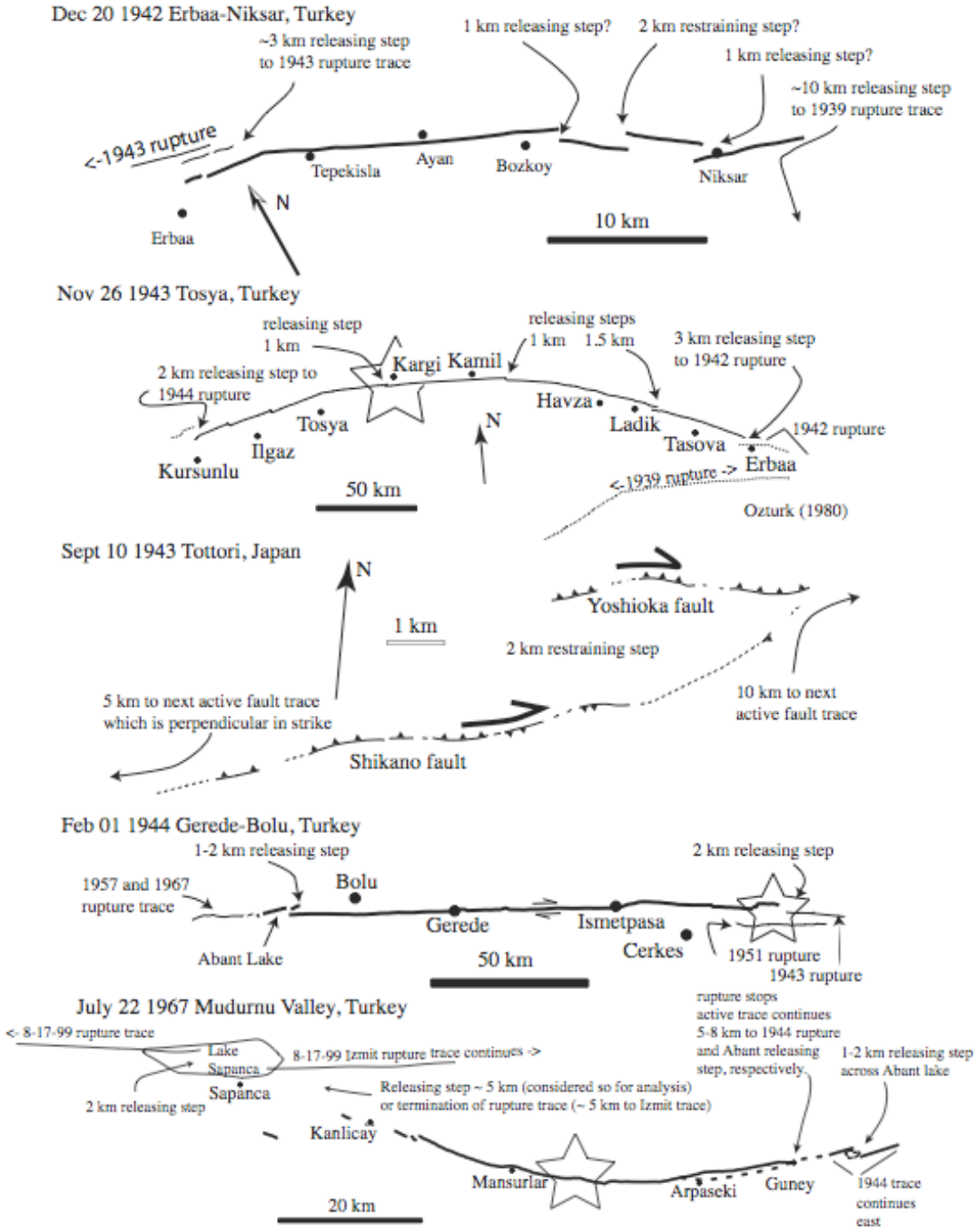

Figure 1a (continued)

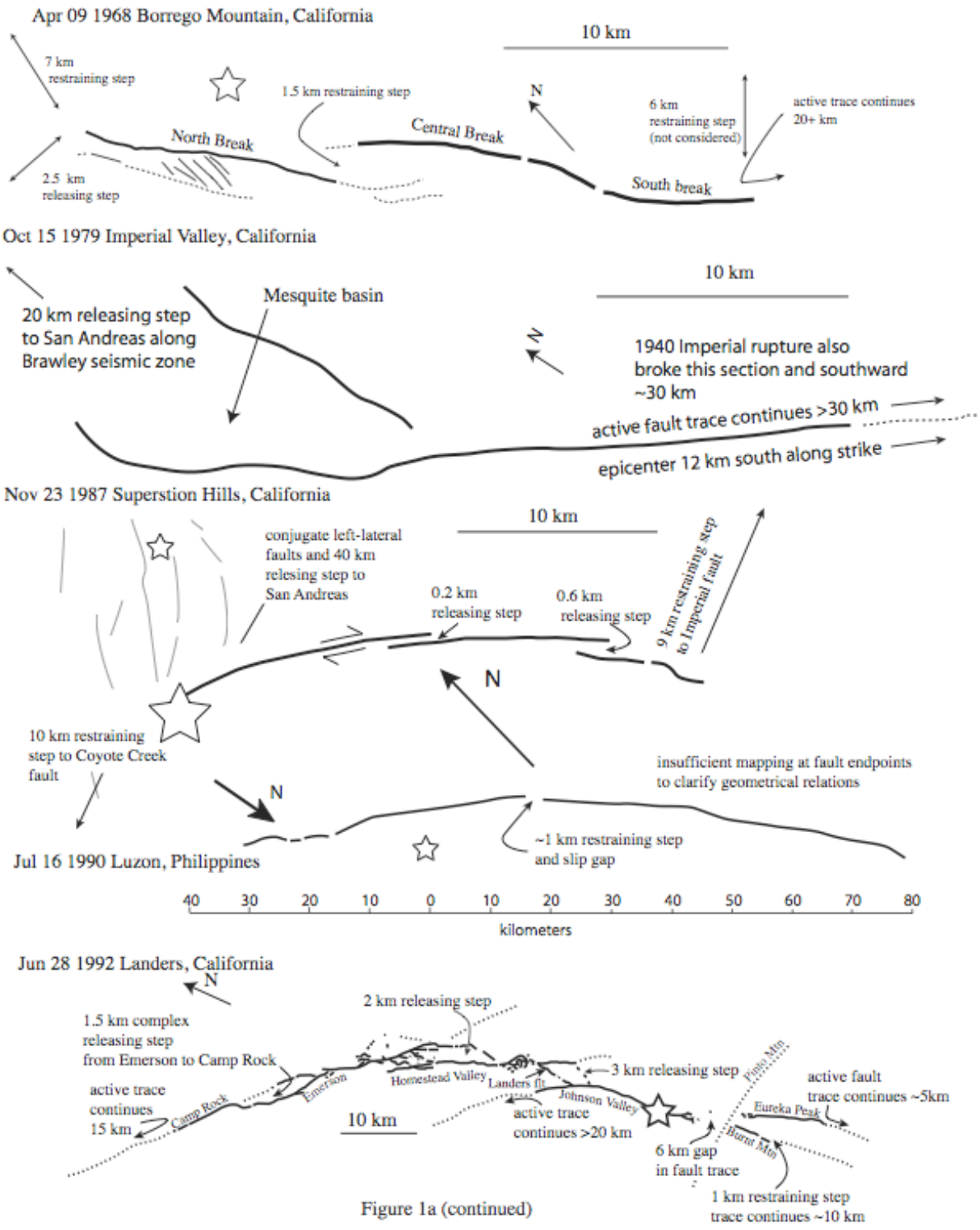

Figure 1a (continued)

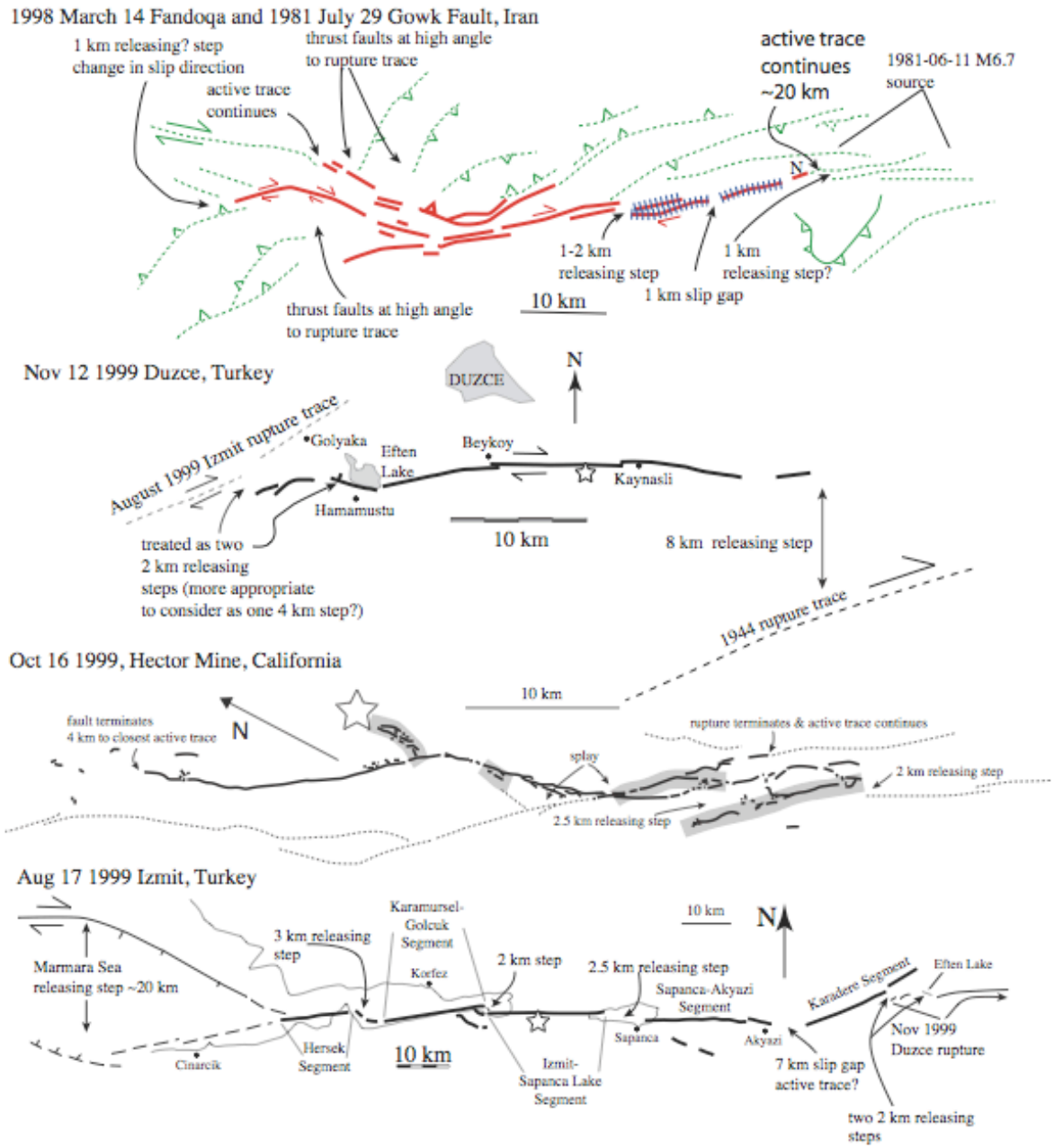

Figure 1a (continued)

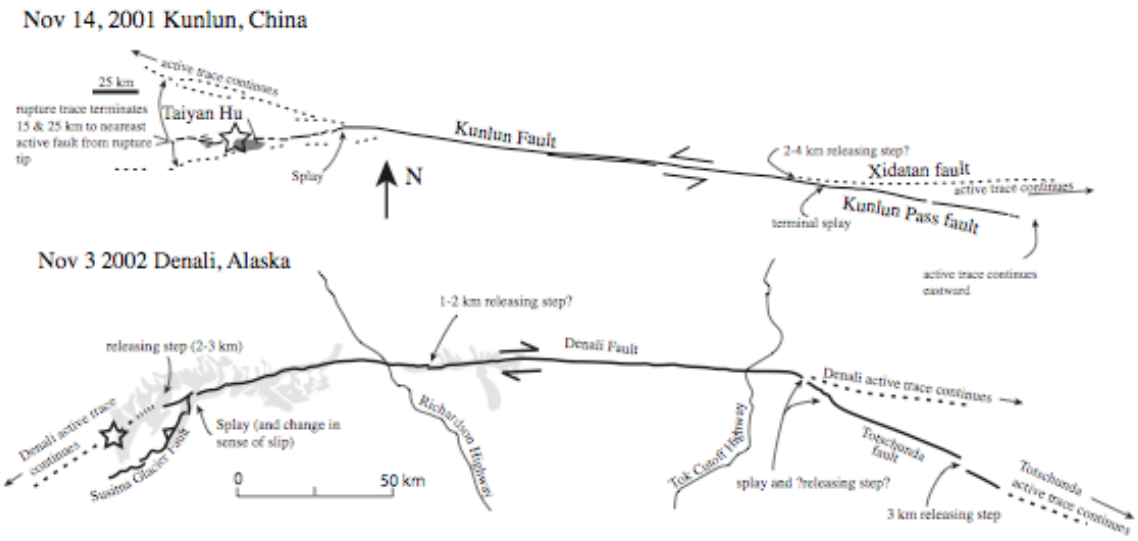

Figure 1a (continued)

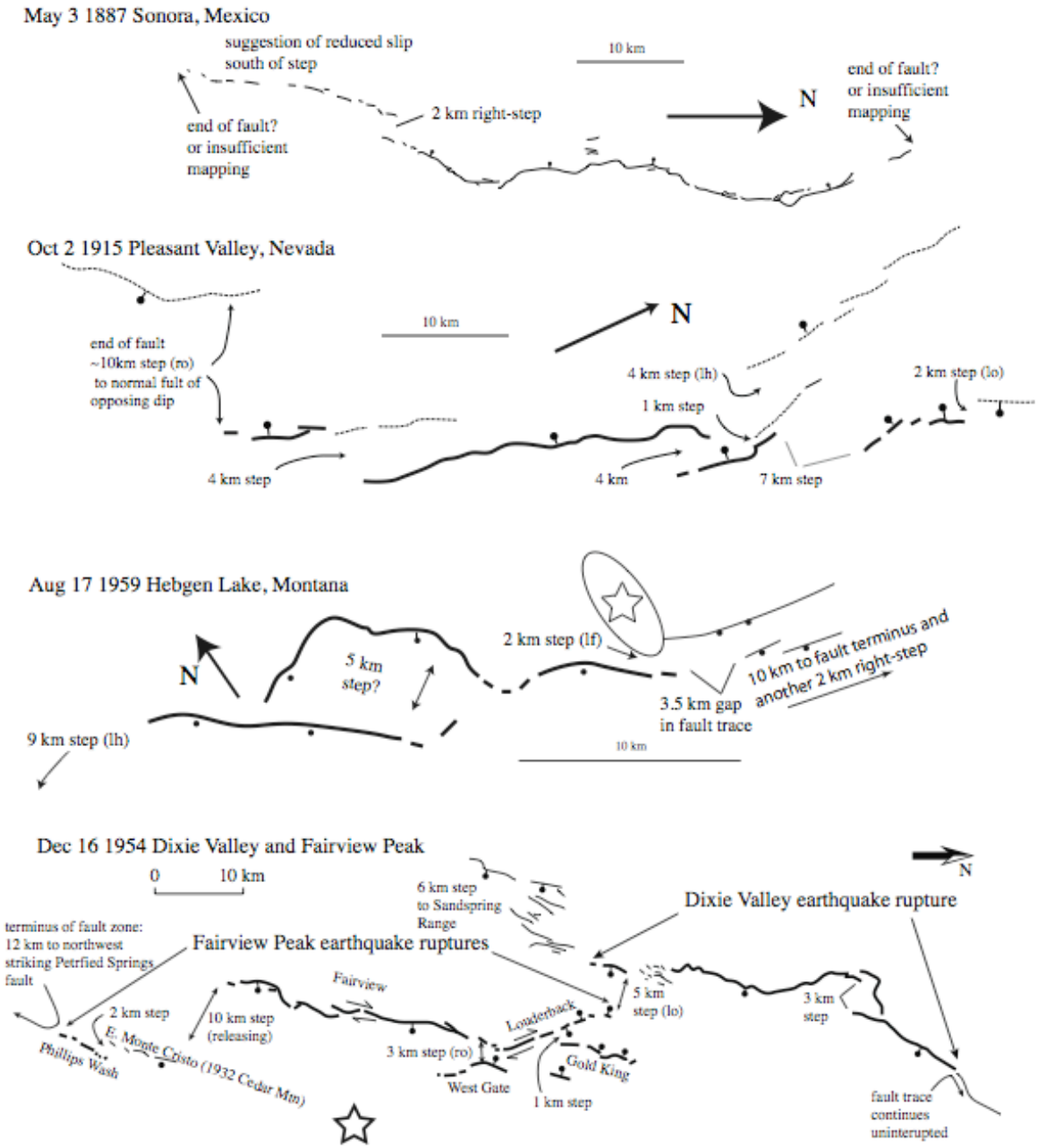
May 3 1887 Sonora, Mexico
suggestion of reduced slip south of step
10 km
end of fault? or insufficient mapping
2 km right-step
N
end of fault? or insufficient mapping
Oct 2 1915 Pleasant Valley, Nevada
10 km
N
end of fault ~10km step (ro) to normal fult of opposing dip
4 km step (lh)
2 km step (lo)
1 km step
4 km step
4 km
7 km step
Aug 17 1959 Hebgen Lake, Montana
N
5 km step?
2 km step (lf)
10 km to fault terminus and another 2 km right-step
3.5 km gap in fault trace
9 km step (lh)
10 km
Dec 16 1954 Dixie Valley and Fairview Peak
0
10 km
N
6 km step to Sandspring Range
Dixie Valley earthquake rupture
terminus of fault zone: 12 km to northwest striking Petrfied Springs fault
Fairview Peak earthquake ruptures
Fairview
2 km step
10 km step (releasing)
Loderback
5 km step (lo)
3 km step
Phillips Wash
E. Monte Cristo (1932 Cedar Mtn)
3 km step (ro)
West Gate
Gold King
1 km step
fault trace continues uninterupted

Figure 1b

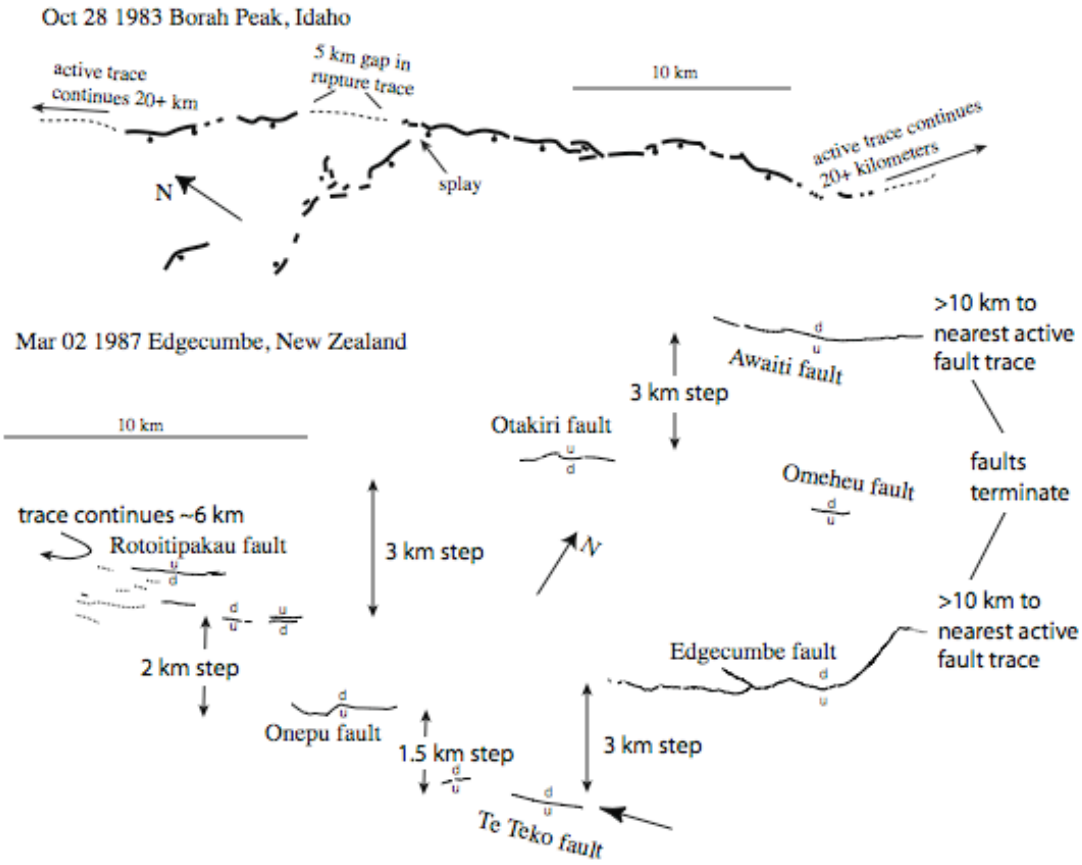

Figure 1b (continued)

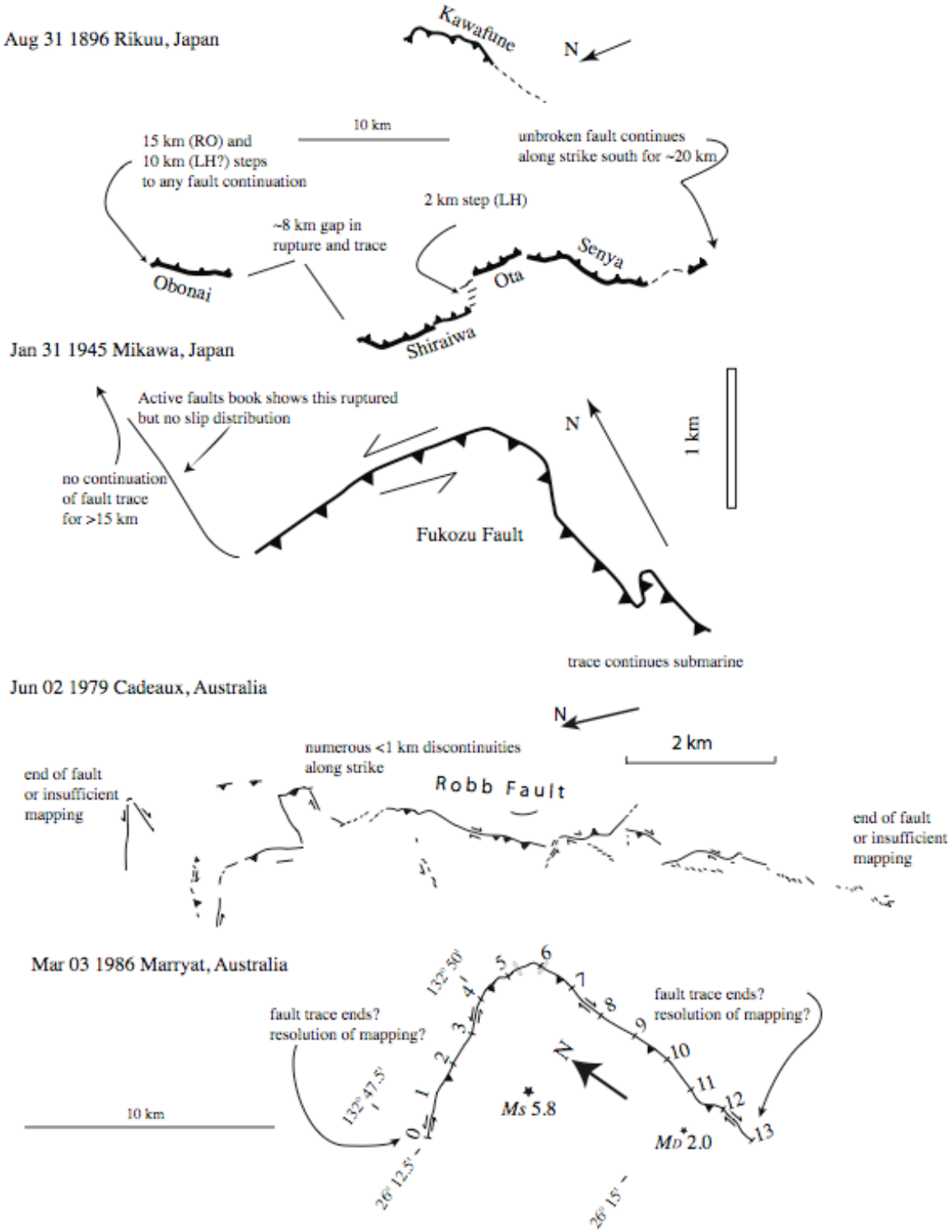
Aug 31 1896 Rikuu, Japan
Kawafune
N
10 km
15 km (RO) and
10 km (LH?) steps
to any fault continuation
unbroken fault continues
along strike south for ~20 km
2 km step (LH)
~8 km gap in
rupture and trace
Senya
Ota
Obonaj
Shiraiwa
Jan 31 1945 Mikawa, Japan
Active faults book shows this ruptured
but no slip distribution
N
1 km
no continuation
of fault trace
for >15 km
Fukozu Fault
trace continues submarine
Jun 02 1979 Cadeaux, Australia
N
2 km
numerous <1 km discontinuities
along strike
end of fault
or insufficient
mapping
Robb Fault
end of fault
or insufficient
mapping
Mar 03 1986 Marryat, Australia
132° 50'
fault trace ends?
resolution of mapping?
fault trace ends?
resolution of mapping?
N
10 km
132° 47.5'
Ms 5.8
Mb 2.0
26° 12.5'
26° 15'
0
1
2
3
4
5
6
7
8
9
10
11
12
13

Figure 1c

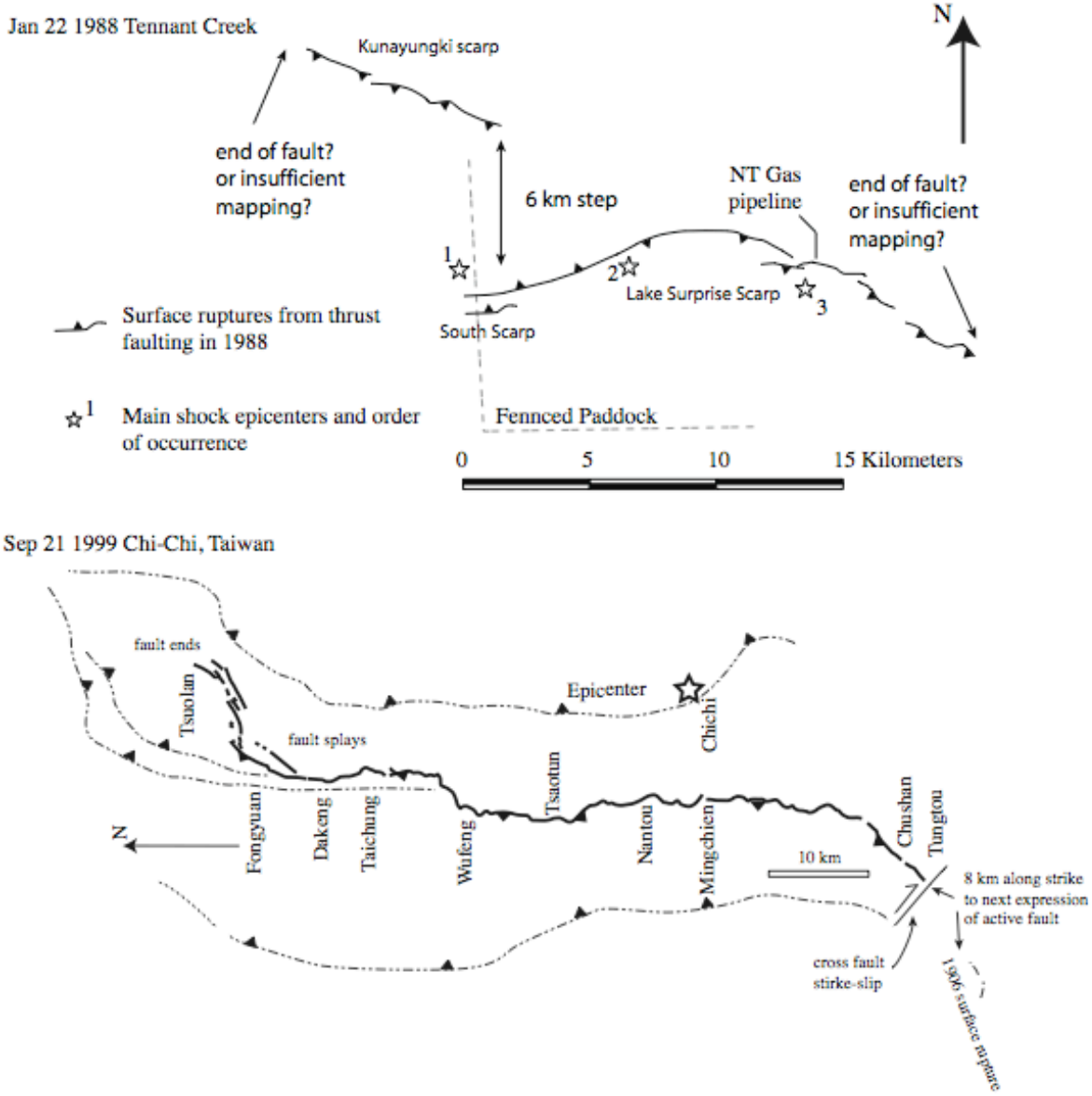

Figure 1c (continued)

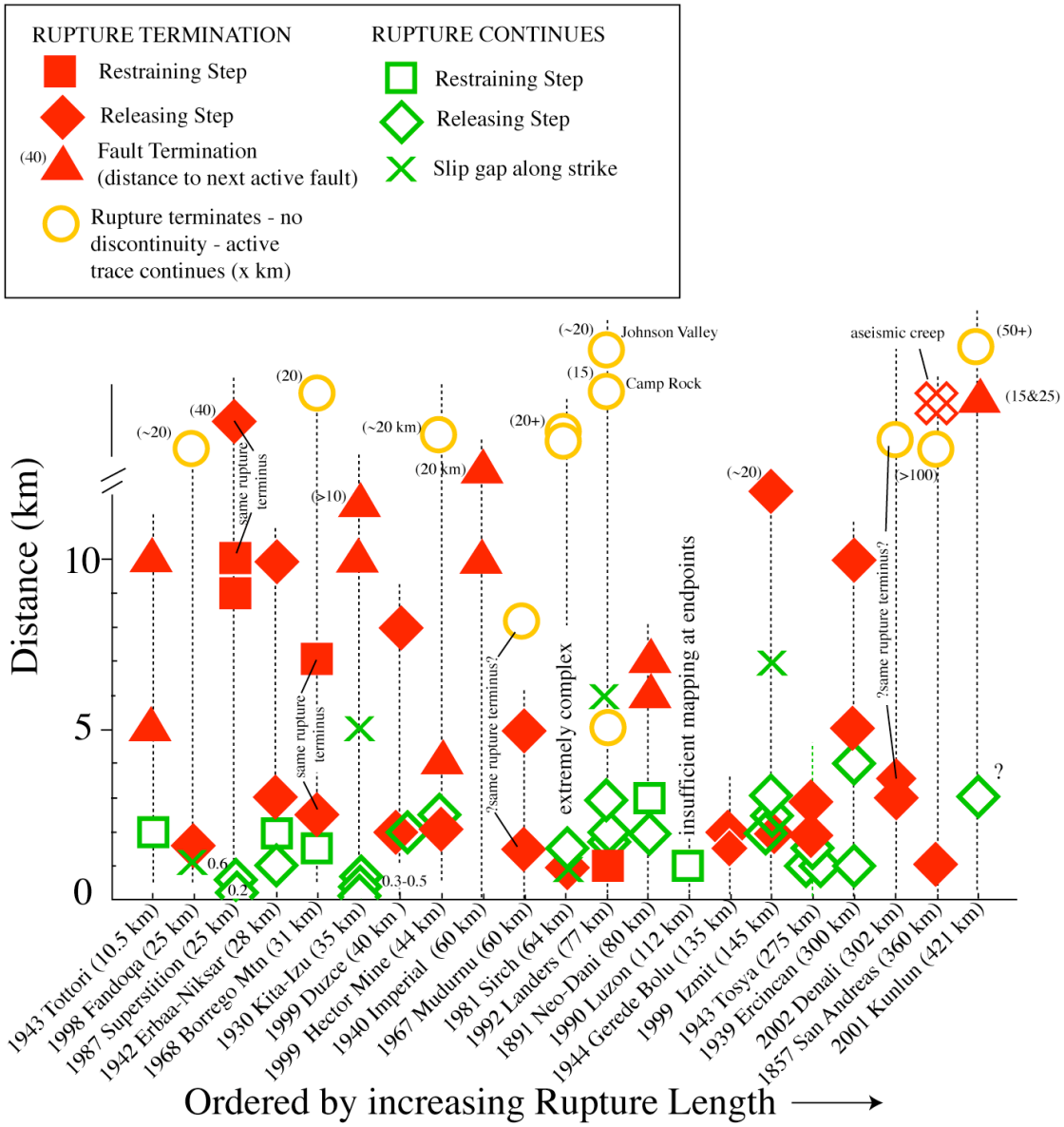

Figure 2. Relationship between the length of earthquake surface rupture and geometrical discontinuities along strike for strike-slip earthquakes. See text for full discussion and description.

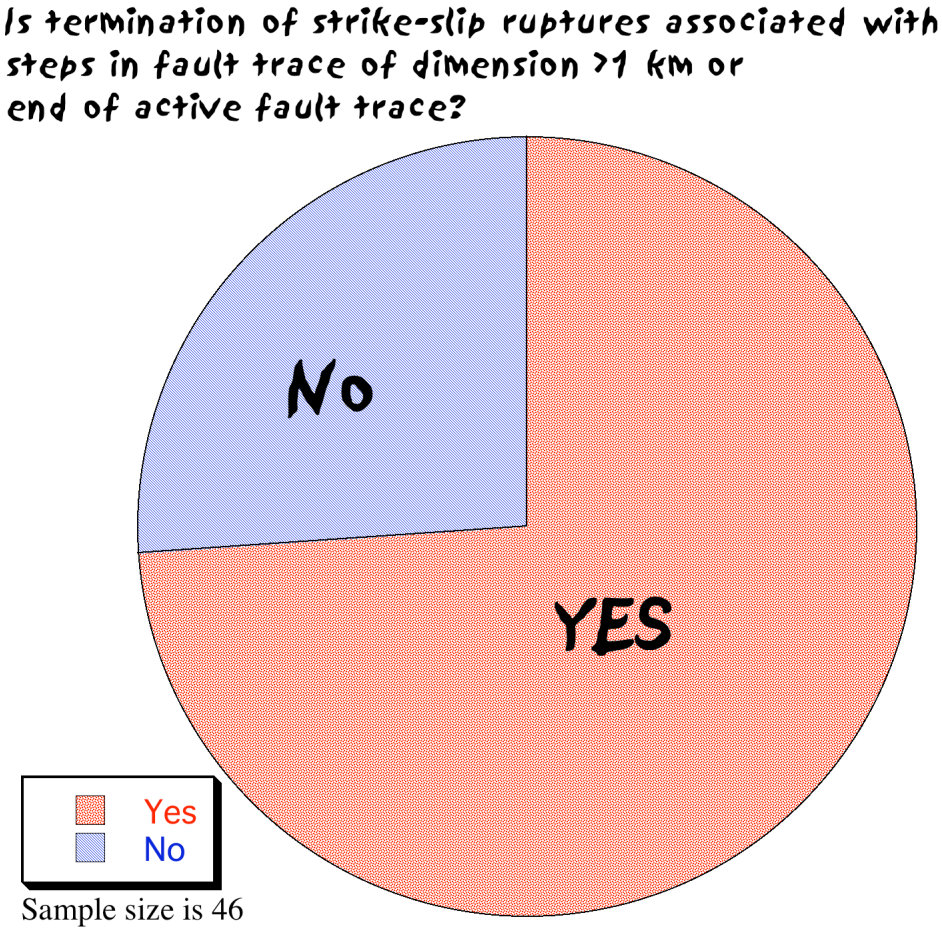

Figure 3. Pie diagram illustrating the relative number of earthquake ruptures with ends at points of geometrical complexity: steps in fault trace of dimension >1km or the end of active fault traces.

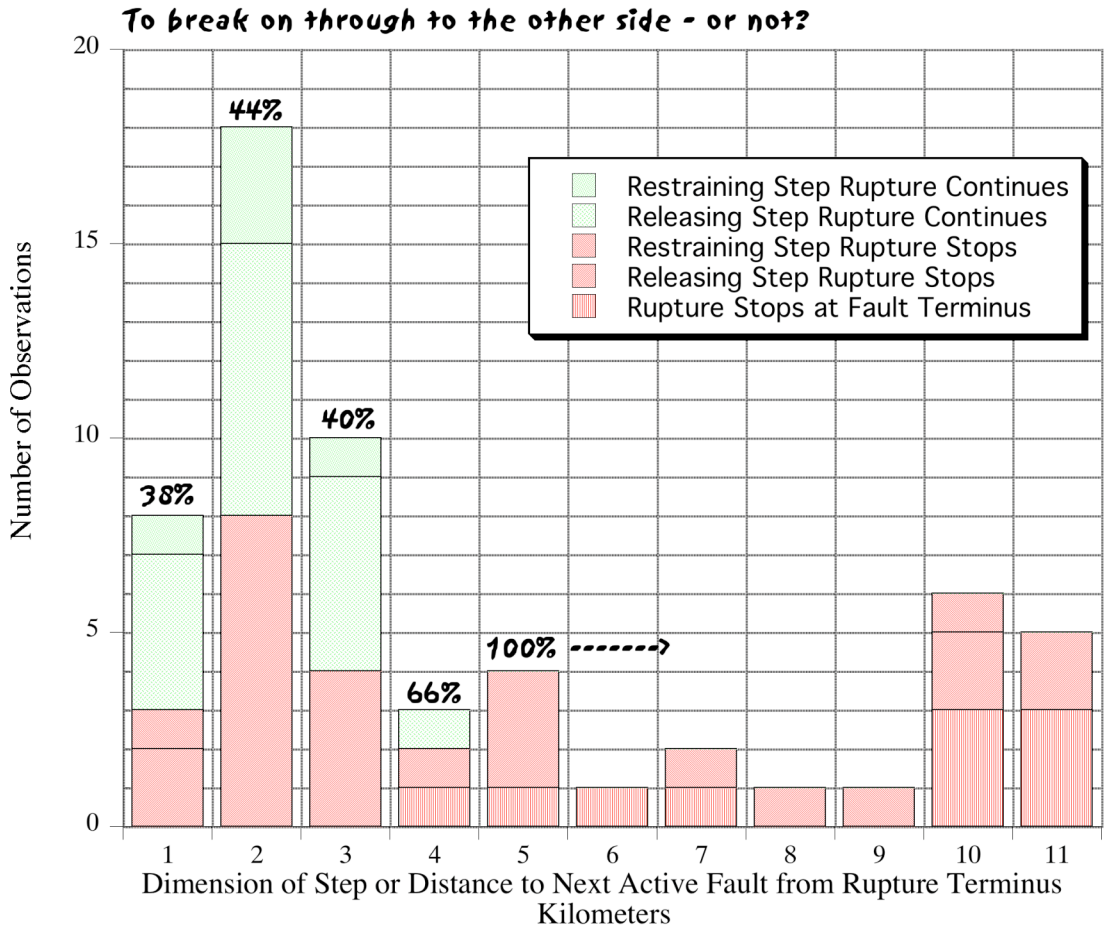

Figure 4. Histogram shows observed number of discontinuities through which earthquakes ruptured (green) and at the end of historical strike-slip earthquakes as a function of the dimension of the discontinuity. Discontinuities are measured as steps in fault trace greater than or equal to 1 km perpendicular to fault strike or, in the case of rupture endpoints, the closest distance to the nearest neighboring active fault.

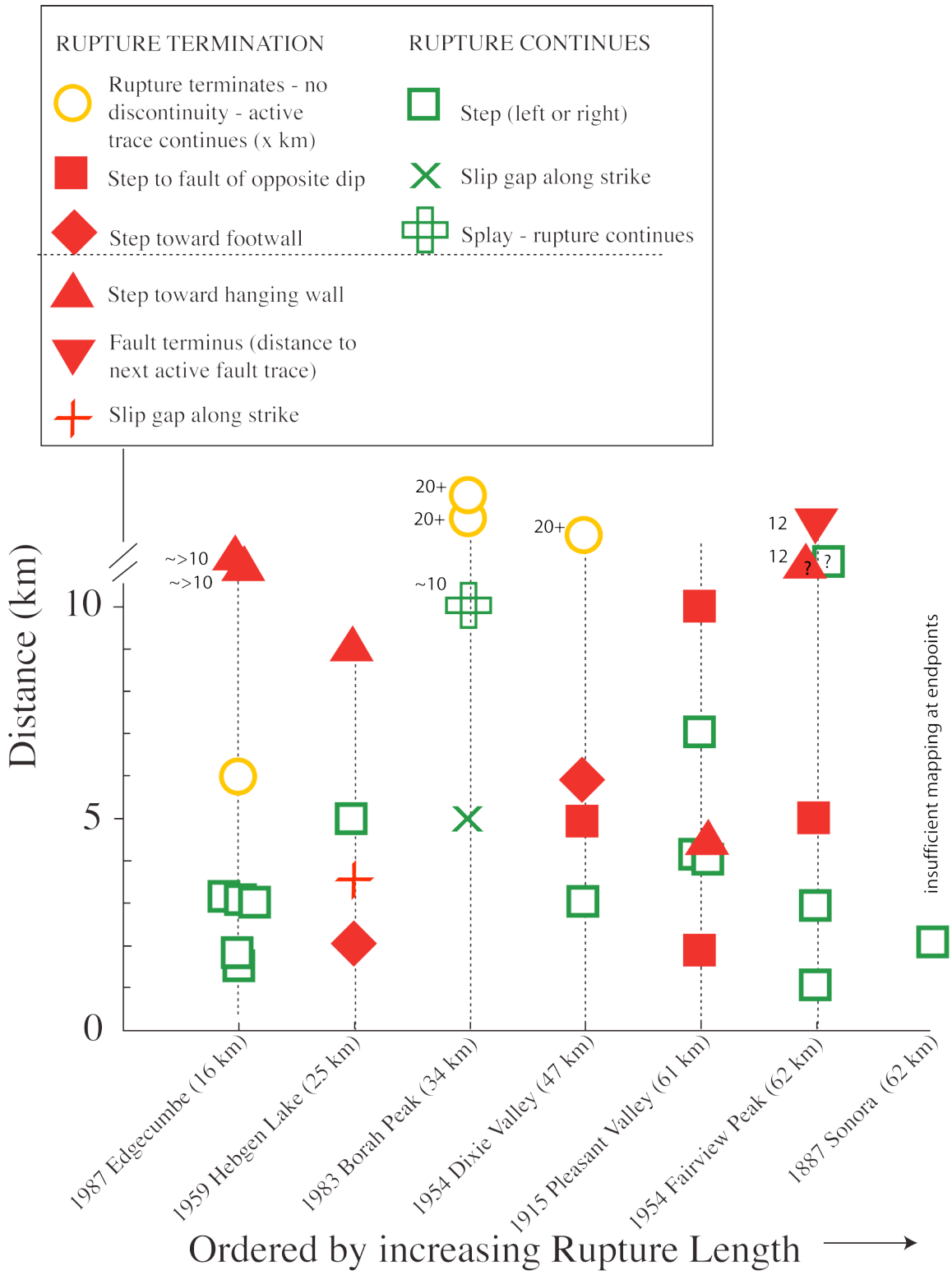

Figure 5. Relationship between the length of earthquake surface rupture and geometrical discontinuities along strike for normal earthquakes. See text for full discussion and description.

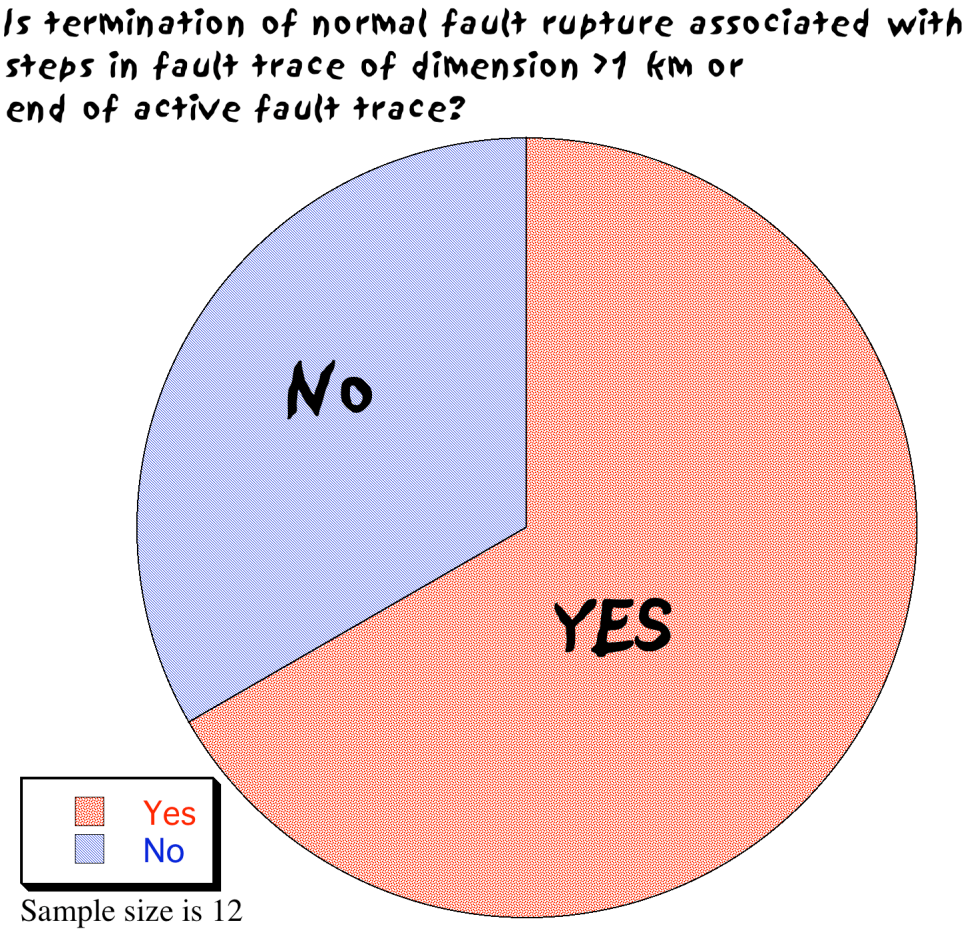

Figure 6. Pie diagram illustrating the relative number of normal mechanism earthquake ruptures with ends at points of geometrical complexity: steps in fault trace of dimension >1km or the end of active fault traces.

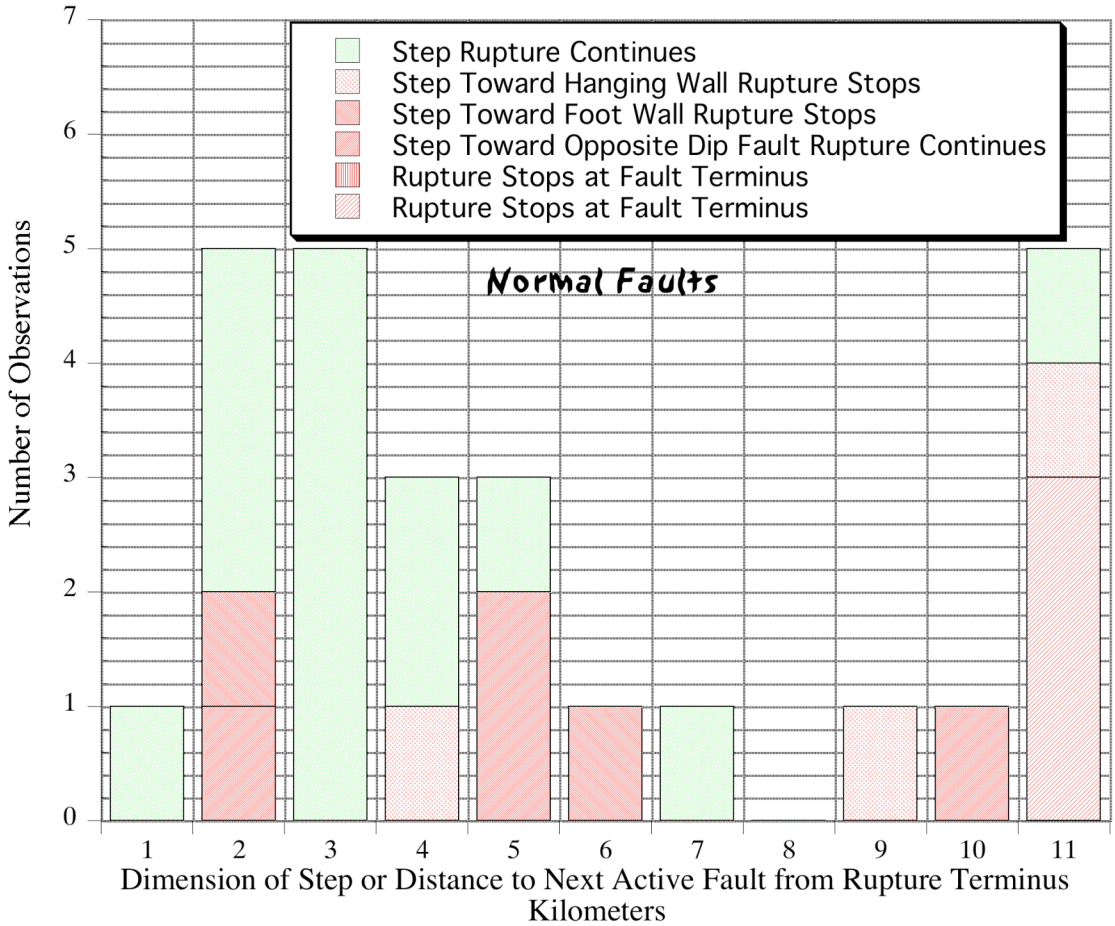

Figure 7. Relationship between the length of earthquake surface rupture and geometrical discontinuities along strike for earthquakes on normal faults. See text for full discussion and description.

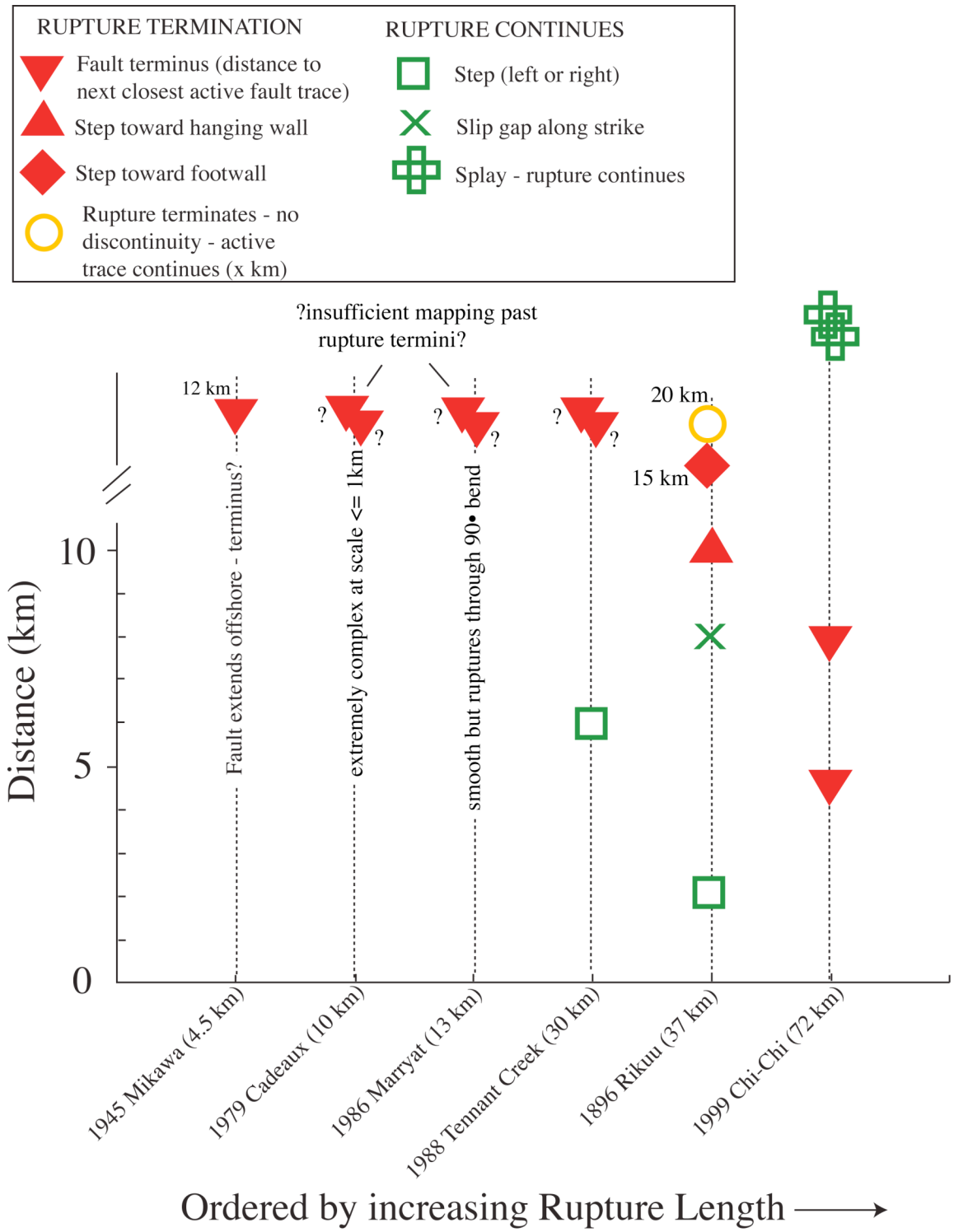

Figure 8. Relationship between the length of earthquake surface rupture and geometrical discontinuities along strike for thrust earthquakes. See text for full discussion and description.

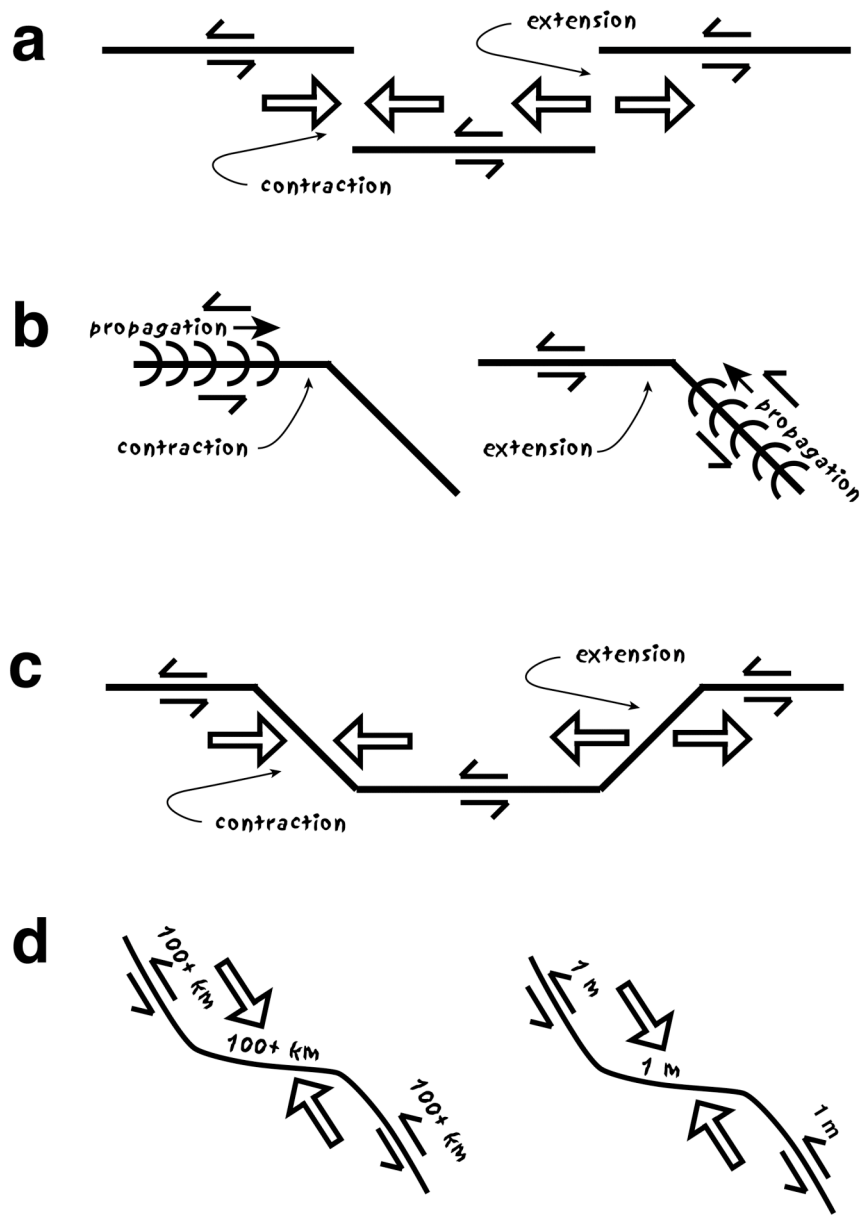

Figure 9. a) Volumetric considerations at steps in fault strike along strike-slip faults leads to localized areas of extension or contraction that may affect earthquake rupture propagation. b) Schematic illustrates that the occurrence of localized compression or extension at a fault bend may be dependent on the direction of rupture propagation. c) Where the direction of preferred pure strike-slip along a fault is well defined (solid half arrows), sections of fault between the bends and oblique to the preferred direction of slip will be characterized by components of contraction and extension. d) The potential effect of fault bends as illustrated in (b) and (c) on the propagation of a rupture will not be solely a function of the angle of the bend but also the sharpness of the bend and the length of the fault branches between bends.